# Performance Analysis of Intelligent Reflecting Surface aided Cell-free Communications

Khushnub Anwar\*a, Imtiaz Ahmed<sup>b</sup>, Mohammad Abdul Matina, Md Sahabul Alam<sup>c</sup>, Kamrul Hasan<sup>d</sup> aUniversity of Denver, Denver, CO, USA 80210; bHoward University, Washington, DC, USA 20059; cCalifornia State University, Northridge, CA, USA 91330; dTennessee State University, Nashville, TN, USA 37209

### **ABSTRACT**

The next generation of cellular communication networks aims to enable ubiquitous connectivity with limited inter-cell interference through cell-free massive multiple-input multiple-output (CF-MMIMO) technology. Deploying an intelligent reflecting surface (IRS) in the cell-free (CF) architecture can significantly enhance coverage area and increase network spectrum efficiency. The signals reflected from IRS can be superposed coherently at the user by introducing the phaseshift with passive reflecting elements (PREs) on IRS. Non-terrestrial communications via unmanned aerial vehicles (UAVs) are critical in providing the seamless connection of the next generation of cellular communication systems. In the current terrestrial network, the signal strength of aerial platforms like UAVs is compromised as the access points (APs) are, in general, aimed at serving ground user ends (GUEs). This challenge can be addressed by incorporating IRS into the CF-MMIMO network. In this paper, we present an IRS-assisted CF-MMIMO network architecture that provides coverage for conventional terrestrial and evolving non-terrestrial aerial user equipment (UEs) simultaneously. The terrestrial UEs experience Rayleigh fading in this architecture, while the non-terrestrial aerial UEs experience Rician fading. To assess the performance of the considered system intuitively, we derive closed-form expressions for both the downlink (DL) spectral efficiency (SE) and the overall system outage probability. These analytical tools allow us to gain valuable insights into the design of CF systems for the next generation of communication systems. To further demonstrate the effectiveness of our developed analytical framework, we validate the developed theoretical tools with Monte Carlo computer simulations for various use cases of the CF-MMIMO network.

Keywords: Cell-free Communications, MIMO, IRS, UAVs, Outage Probability.

## 1. INTRODUCTION

Faster data rates, better spectrum efficiency, and seamless connectivity are becoming more and more in demand in the dynamic world of wireless communication technologies. "Cell-Free Massive MIMO" (CF-MMIMO) has been developed as a possible solution to improve the performance of wireless networks in order to meet these objectives. CF-MIMO, which integrates dispersed antennas and cooperative processing, offers considerable benefits over traditional Multiple-Input Multiple-Output (MIMO) systems. By shifting away from the conventional cellular framework, this innovative strategy gives wireless networks more flexibility, coverage, and user-friendly capabilities. According to recent studies, CF networks perform better than traditional cellular and small cell networks<sup>1</sup>, indicating that they will be a strong candidate for emerging wireless network technologies.

As a cutting-edge strategy to transform wireless communication networks, "Intelligent Reflecting Surfaces" (IRSs) have recently attracted a lot of attention. An IRS comprises of an extensive number of passive reflecting elements (PREs) that may be modified to provide an incoming signal with different phase shifts. The possible data rates are increased as an outcome of this modification and the propagation of signals is also enhanced<sup>2</sup>.

IRS shows great potential for improving signal reception, reducing interference, and expanding coverage by precisely altering the phase and amplitude of incoming electromagnetic waves. The prospective effects of IRS on wireless communication are significant since they have the power to fundamentally alter how networks operate at present.

Recently, the use of IRSs has been investigated to improve Unmanned Aerial Vehicle (UAV) communication in a variety of settings<sup>[3,4]</sup>. Studies indicated that incorporating an IRS may significantly increase the strength of the signal received by UAVs that can broaden the coverage range. With the flexibility to modify the wireless channel to meet expected communication requirements, IRS creates a wide range of opportunities for wireless systems to achieve previously unattainable standards of performance, efficiency, and connection. In the development of smart radio environment for the future sixth generation (6G) of wireless communication systems, IRSs have a great potential and a significant amount of curiosity and interests have been drawn towards it<sup>5</sup>.

A theoretical model that demonstrates the ideal phase-shift configuration for achieving a high signal-to-noise ratio (SNR) for the synthesized received signal has been presented<sup>6</sup>. IRS-assisted models also has some challenges including the primary user being affected from the interference occurred by another user.<sup>7</sup>

In this paper, we analyze IRS-incorporated CF-MMIMO system. We thoroughly investigated and examined several characteristics of our model including the Cumulative Distribution Function (CDF) and Probability Density Function (PDF) in a multi-user scenario with an IRS panel between the source and destination. For our proposed model, we also derived the expression of Outage Probability (OP) and used MATLAB evaluate the results numerically.

### 2. SYSTEM MODEL

We consider an IRS-integrated CF system where multiple M APs are serving multiple Ground User Equipment (GUEs) and we aim to evaluate the performance of one of the GUEs denoted by D. The IRS panel contains Q number of PREs that direct the signal to the intended destination D. The channel coefficients for the channel gains from source 1 to M to the IRS panel are denoted by  $h'_{1q}, h'_{2q}, \dots h'_{Mq}$ . The channel coefficients for the direct link from M sources to destination D are denoted by  $h'_{01}, h'_{02}, \dots h'_{0M}$ . Let,  $h'_{0m}$  denote the coefficients for the channel from the m-th source to user D directly and  $h'_{mq}$  denote the channel coefficient from the m-th source to the IRS Panel on its q-th element.  $b'_q$  indicates the channel coefficient from the q-th element of the IRS panel to one of the users denoted by D. If we denote the phases of  $h'_{0m}, h'_{mq}$ , and  $h'_q$  by  $\emptyset_{0m}, \emptyset_{mq}$  and  $\Psi_q$  respectively, then the polar form for the channel coefficients can be expressed as:  $h'_{0m} = h_{0m}e^{j\emptyset mq}$ ,  $h'_{mq} = h_{mq}e^{j\emptyset mq}$ ,  $b'_q = b_q e^{j\Psi q}$ .

Now,  $\varrho = diag([k_1e^{j\theta 1},\dots,k_qe^{j\theta q},\dots k_Qe^{j\theta Q}])$  represent the phase-shift matrix<sup>8</sup>. Here,  $k_q \in (0,1]$  and  $\theta_q \in [0,2\pi)$  are the amplitude reflection coefficient and the phase shift of the q-th reflecting element of the IRS, respectively.

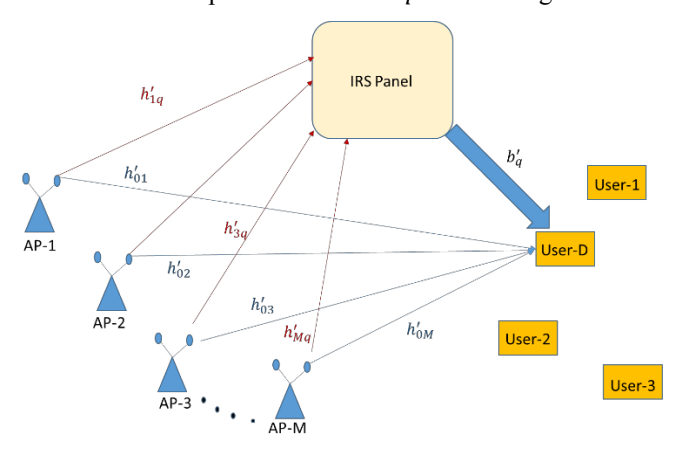


Figure 1: Visual Illustration of the System Model. Access points are indicated by AP.

Fig. 1 presents the system model in detail where the channel coefficients are indicated for each type of propagation. We are analyzing the performance of the user denoted by D in a multi-user environment. In our work, It is anticipated that the controllers of the IRS and the source considered both have knowledge of the ideal global channel state information. Now, the received signal at user D will be the summation of all the signals from all the APs (m = 1 to m = M) that directly reaches the user and the reflected signal from the IRS which can be written as using coherent combination<sup>[9,10,11]</sup>.Let us denote the received signal at the destination by  $Y_{RX}$ ,

$$Y_{Rx} = \sum_{m=1}^{M} \sqrt{P_m (h_{om} + \sum_{q=1}^{Q} b_q k_q e^{j\theta q} h_{mq}) x_m + n}$$
 (1)

Here,  $x_m$  is considered to be the transmitted signal from each Access Point (AP) and  $P_m$  is the transmit power in dBm which we consider to be equal for all the sources in our model. In addition, n is the Additive White Gaussian noise (AWGN) at D with zero mean and variance  $\sigma^2$  i.e.,  $n \sim \text{CN}(0, \sigma^2)^{11}$ . Equation (1) can be represented as a function of the SNR for our system by following the steps in  $n \sim \text{CN}(0, \sigma^2)^{11}$ .

$$SNR_{D} = \left| \sum_{m=1}^{M} \tau_{m} \left( h_{om} e^{j\varphi_{0m}} + \sum_{q=1}^{Q} b_{q} k_{q} h_{mq} e^{j(\theta_{q} + \varphi_{mq} + \Psi_{q})} \right) \right|^{2} . \tag{2}$$

After some mathematical manipulations, SNR can be simplified as written below:

$$SNR_{D} = \left| e^{j\varphi_{0m}} \right|^{2} \left| \sum_{m=1}^{M} \tau_{m} \left( h_{0m} + \sum_{q=1}^{Q} b_{q} k_{q} h_{mq} e^{j\delta_{q}} \right) \right|^{2} . \tag{3}$$

In equation (3),  $\delta_q = \theta_q + \varphi_{mq} + \Psi_q - \varphi_{0m}$  is considered as the Phase Error in case of the q-th element of the IRS panel utilized in the model.

$$SNR_{D} = \left| \sum_{m=1}^{M} \tau_{m} \left( h_{om} + \sum_{q=1}^{Q} b_{q} k_{q} h_{mq} e^{j\delta_{q}} \right) \right|^{2} . \tag{4}$$

The average transmit SNR is represented by,  $\tau_m = P_m/\sigma^2$ . The desired phase-shift configuration of the q- th reflecting element contained in the IRS may be described mathematically as  $\ddot{\Theta} = \varphi_{om} - (\varphi_{mq} + \Psi_q)^{11}$ . As a result, the amplitude of the synthesized received signal at position D becomes the highest. If we consider  $|e^{j\varphi_{om}}|^2 = 1$ , the final expression for SNR at D can be thus written as

$$SNR_D = \left| \sum_{m=1}^{M} \tau_m \left( h_{0m} + \sum_{q=1}^{Q} b_q k_q h_{mq} \right) \right|^2 . \tag{5}$$

#### 3. OUTAGE PROBABILITY

In this section, we obtain OP for the downlink CF communication system where a user is being served by multiple APs via IRS. We discuss both Nakagami distribution and Gamma distribution for our system and use Gamma Distribution for the obtaining the plot of the PDF and CDF. Both distribution were analyzed and expression for OP was obtained. The PDF and CDF of the Nakagami-m are described by the parameters m and  $\Pi^{12}$ . Suppose there are two separate random variables (RVs), H1 and H2, both of which have Nakagami-H2 distributions. H1 is Nakagami (H3, H4, while H4 is Nakagami (H5, H4, while H6 is Nakagami (H5, H6, while H8 is Nakagami (H8, H9, H9, while H9 is Nakagami (H9, H9, while H9 is Nakagami

$$f_X(x; m, \Pi) = \frac{2m^m}{\Gamma(m)\Pi^m} x^{2m-1} e^{-\frac{m}{\Pi}x^2}$$
 (6)

and 
$$F_X(x; m, \Pi) = \gamma(\frac{m, \frac{m}{n}x^2}{\Gamma(m)})$$
, respectively. (7)

In the above expressions, m > 0 is the shape parameter and  $\Lambda > 0$  is the spread parameter of the distribution. Now, we use the alternative representation for denoting a Nakagami-m RV:  $X \sim Nakagami$  ( $m, \Lambda$ ). The sign  $\Lambda$  stands for the average channel (power) gain, which is the mean square value of  $X^{13}$ . The distribution of the magnitude of each channel can be demonstrated by the following expressions:

$$h_{0m} \sim Nakagami(m_{0m}, \Pi_{0m}),$$
  $h_{mq} \sim Nakagami(m_{hm}, \Pi_{hm}),$  and  $b_a \sim Nakagami(m_{hg}, \Pi_{hg}).$ 

Let, Y be a RV following a Gamma distribution, whose PDF and CDF, parameterized by  $\delta$  and  $\omega$ , respectively given by  $^{12}$ 

$$f_Y(y;\delta,\omega) = \frac{\omega^{\delta}}{\Gamma(\delta)} y^{\delta-1} e^{-\omega y}, y \ge 0,$$
 (8)

and 
$$F_Y(y; \delta, \omega) = \frac{\gamma(\delta, \omega y)}{\Gamma(\delta)}, y \ge 0$$
, respectively. (9)

We define the following terms or symbols for notational convenience:  $J_{mq} \triangleq b_q k_q h_{mq}$ ,  $V_m \triangleq \sum_{q=1}^Q J_{mq}$ ,  $L = \sum_{m=1}^M V_m$ . The following RV will be used to indicate the magnitudes of the end-to-end channel coefficients in our model where  $U \triangleq \sum_{m=1}^M h_{om} + L = H_{om} + L$ .

The exact PDF of  $J_{mq}$  is expressed as<sup>11</sup>:

$$f_{J_{mq}}(u) = \frac{4\xi_{mq}^{mh_m + m_{b_q}}}{\Gamma_{m_{h_m}} \Gamma_{m_{b_q}}} x^{m_{h_m} + m_{b_q} - 1} K_{m_{b_q} - m_{h_m}} (2\xi_{mq} U), \tag{10}$$

where,  $\xi_{mq} = \sqrt{\frac{m_{h_m} m_{b_q}}{K^2 q \, \Pi_{h_m} \, \Pi_{b_q}}}$ . We obtain this PDF of  $J_{mq}$  by inserting values in  $f_{XY}(u) = \int_0^\infty \frac{1}{x} \, f_Y \, \frac{u}{x} \, f_X(x) dx$  and the mathematical calculations from the work conducted in  $I_{qq}^{14}$ .

It can be observed that  $J_{mq}$  follows a  $K_G$  distribution having the shaping parameters denoted by  $m_{bq}$  and  $m_{hm}$ . By utilizing the exact PDF of  $J_{mq}$ , the k-th moment of  $J_{mq}$  can be obtained after a few mathematical modifications, defined as  $\eta_{imq}(k)$ , the k-th moment can be obtained as:

$$\eta_{J_{mq}}(k) = \xi_{mq}^{-k} \frac{\lceil m_{h_m} + \frac{k}{2} \lceil m_{b_q} + \frac{k}{2} \rceil}{\lceil m_{h_m} \rceil m_{b_m}} . \tag{11}$$

For the IRS with 1,..., Q reflecting elements, the  $J_{mq}$  random variables are i.i.d. to a Gamma distribution with respect to the reflecting elements if M is provided. Thus, we obtain  $J_{mq}$ ,

$$J_{mq} \approx Gamma(\delta J_m, \omega j_m),$$
 (12)

where, 
$$\delta J_m = \frac{(E[J_{mq}])^2}{Var[J_{mq}]} = \frac{[\eta_{Jmq}(1)]^2}{\eta_{Jmq}(2) - [\eta_{Jmq}(1)]^2}$$
 and  $\omega j_m = \frac{E[J_{mq}]}{Var[J_{mq}]} = \frac{\eta_{Jmq}(1)}{\eta_{Jmq}(2) - [\eta_{Jmq}(1)]^2}$ .

We can represent the approximate distribution of  $V_m$  as 11:

$$V_m \approx Gamma(Q\delta J_m, \omega J_m).$$

As a result, the following expressions provide the approximate CDF and PDF of  $V_m$ 

$$F_{V_m}(u) \approx \frac{\gamma(Q\delta_{Jm},\omega_{Jm}U)}{\Gamma(Q\delta_{Jm})} \tag{13}$$

and 
$$f_{V_m}(u) \approx f_{V_m}(u; Q\delta_{Im}, \omega_{Im})$$
, respectively. (14)

Now using Multinomial Expansion approach in  $^{1410}$ , the k-th moment of  $V_m$  can be written considering the calculations in  $^{11}$  as,

$$\eta_{V_{m}}(k) = \sum_{k_{1}=0}^{K} \sum_{k_{2}=0}^{K} \dots \dots \sum_{k_{Q-1}=0}^{k_{Q-2}} {k \choose k_{1}} {k \choose k_{2}} \dots \dots {k_{Q-2} \choose k_{Q-1}} \times \eta_{J_{m_{1}}}(k-k_{1}) \times \eta_{J_{m_{2}}}(k_{1}-k_{2}) \dots \dots \times \eta_{J_{m_{Q}}}(k_{Q-1}) . \tag{15}$$

Now, as  $L = \sum_{m=1}^{M} V_m$ , we can obtain the k-th moment of L through a similar approach,

$$\eta_{L}(k) = \sum_{k_{1}=0}^{K} \sum_{k_{2}=0}^{K} \dots \sum_{k_{M-1}=0}^{K} \binom{k}{k_{1}} \binom{k_{1}}{k_{2}} \dots \binom{k_{M-2}}{k_{M-1}} \times \eta_{V_{1}}(k-k_{1}) \times \eta_{V_{2}}(k_{1}-k_{2}) \dots \times \eta_{V_{m}}(k_{M-1}).$$

$$(16)$$

From  $\eta_{V_m}(k)$ ,  $\eta_L(k)$  and  $\eta_{I_{ml}}(k)$  we can calculate the first and second moment of L for M sources and one IRS,

$$\eta_L(1) = \sum_{m=1}^{M} \sum_{q=1}^{Q} \eta_{Imq}(1) \tag{17}$$

$$\eta_{L}(2) = \sum_{m=1}^{M} \left[ \sum_{q=1}^{Q} \eta_{Jmq}(2) + 2 \sum_{q=1}^{Q} \eta_{Jmq}(1) \sum_{q'=q+1}^{Q} \eta_{J_{mq'}}(1) \right] + 2 \sum_{m=1}^{M} \left[ \sum_{q=1}^{Q} \eta_{Jmq}(1) \right] \sum_{m'=m+1}^{M} \left[ \sum_{q=1}^{Q'} \eta_{J_{mq'}}(2) \right]. \tag{18}$$

Now, using the binomial theorem for  $U \triangleq \sum_{m=1}^{M} h_{om} + L = H_{om} + L$ , we can write,

$$\eta_u(k) = \sum_{q=0}^k \binom{k}{q} \eta_{Hom}(q) \eta_L(k-q) \quad . \tag{19}$$

From the above equation we have,

$$\eta_u(1) = \eta_{Hom}(1) + \eta_L(1) \tag{20}$$

$$\eta_u(2) = \eta_{Hom}(2) + \eta_L(2) + 2\eta_{Hom}(1)\eta_L(1) \tag{21}$$

The values of  $\eta_{Hom}(1)$  and  $\eta_{Hom}(2)$  are obtained as:

$$\eta_{Hom}(1) = \frac{\Gamma\left(m_o + \frac{1}{2}\right)}{\Gamma m_o} \left(\frac{m_o}{\Lambda_o}\right)^{-1/2} \tag{22}$$

and 
$$\eta_{Hom}(2) = \frac{\Gamma(m_o + 1)}{\Gamma m_o} \left(\frac{\Pi_o}{m_o}\right) = \Pi_o$$
, respectively. (23)

Putting the values of  $\eta_{Hom}(1)$  and  $\eta_{Hom}(2)$  we can obtain  $\eta_u(1)$  and  $\eta_u(2)$  to calculate  $\delta_u$  and  $\omega_u$  by following the calculations in <sup>11</sup>. The PDF and CDF of  $U^2$  can be obtained as

$$f_{U^2}(x) \approx \frac{\omega u^{\delta u}}{2\sqrt{x} \lceil (\delta u)} (\sqrt{x})^{\delta u - 1} e^{-\omega u \sqrt{x}}$$
, (24)

and 
$$F_{U^2}(x) \approx \frac{\gamma(\delta u, \omega u \sqrt{x})}{\Gamma(\delta u)}$$
, respectively. (25)

 $F_{II^2}(x)$  can be modified in the form of gamma distribution as shown in 15

$$f_g(x;t,c,s) = \frac{\left[\frac{s}{t^c}\right]\left[x^{c-1}\right]}{\Gamma\left[\frac{c}{s}\right]} e^{-\left(\frac{x}{t}\right)^s} , \qquad (26)$$

$$F_g(x;t,c,s) \approx \frac{\gamma(\frac{c}{s'}(\frac{x}{t})^s)}{\Gamma(\delta u)} , \qquad (27)$$

which can be written as by following<sup>11</sup>

$$f_{u^{2}}(x) = \frac{\left[\frac{1}{2}\right] / \left[\left(\omega^{-2}u\right)^{\frac{\delta u}{2}}\right]}{\Gamma\left(\frac{\delta u}{2}\right]} x^{\frac{\delta u}{2} - 1} e^{-\left(\frac{x}{\omega^{-2}u}\right)^{\frac{1}{2}}} . \tag{28}$$

The OP can be defined as the possibility that the mutual information of our proposed model will go below a predetermined spectral efficiency (SE) level<sup>11</sup> which can be denoted by R<sub>th</sub> [b/s/Hz].

$$P_{OP} = Prob(log_2(SNR + 1) < R_{th}) \qquad . \tag{29}$$

The final SNR expression can be utilized to construct an approximate closed-form estimate for the OP of our model. This formulation considers the SNR and the calculations conducted previously which can be written as<sup>11</sup>

$$P_{OP} = \text{Prob}(\tau_{\rm m} U^2 \le \tau_{\rm th}) \approx F_z(\sqrt{\frac{\tau_{\rm th}}{\tau_{\rm m}}})$$
 (30)

Here,  $\tau_{th}=2^{R_{th}}-1$  and the property  $F_{x^2}(x)=F_X\left(\sqrt{x}\right)$ , x>0 has been utilized.

#### 4. NUMERICAL RESULTS

In our considered model, we assume multiple sources transmitting signal to the destination through the utilization of an IRS consisting of Q number of Passive Reflecting Elements. We have used MATLAB to generate the simulation results. The CDF, PDF and System Model were plotted using MATLAB codes. The approach taken on the work published in use utilized and modified according to our model. For the simulation of our model, we have considered 5 sources each transmitting within the same range of power (-5dB to 30dB) and the IRS panel containing 30 reflecting elements. The parameters are chosen according to the table presented below:

Table 1. Simulation Parameters for our Proposed Model

Parameters	Values
Number of Sources	5
Source Locations	(0,0), (20,4), (40,7), (3,8), (40,3)
Destination Location	(100,0)
RIS Location	(60,5)
Amplitude Reflection Coefficient, kq	18
Number of Passive Reflecting Elements in RIS,Q	30
Bandwidth in MHz	108
Carrier Frequency, fin GHz	38
Spectral Efficiency (Targeted), R <sub>th</sub> in [b/s/Hz]	111
Power Density of Thermal Noise in [dBm/Hz]	-1748
Noise Figure in dBm	108
Normalized Spread Parameter	1
Nakagami Shape parameter	~v[2,3] <sup>11</sup>
Antenna Gain in dB	58

Using the above parameters and the values provided in Table 1, the simulation results were obtained for multiple sources. The visual illustration of the location of the sources, IRSs and destination is represented in Fig. 2 where the sources are presented by red circles and the blue square represents the location of the IRS. The coordinate of the destination is (100,0)

shown by the yellow triangle<sup>12</sup>. The average location height for the sources are shown by H(m) and considered to be 10 meters.  $d_{SD}$  shows the distance in meters.

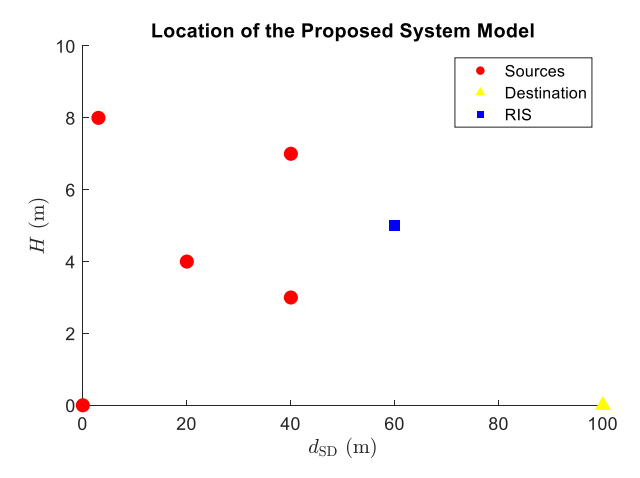


Figure 2: Location of the sources, destination and IRS of the model

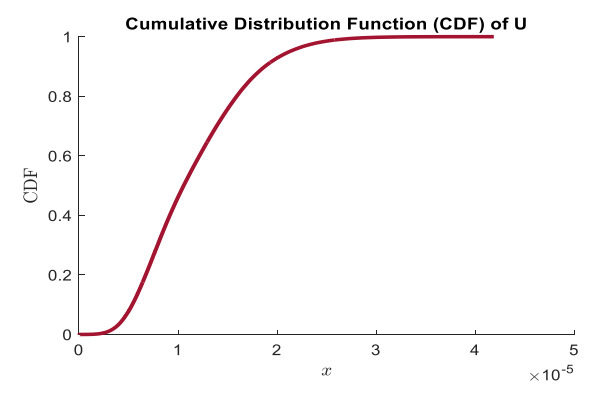


Figure 3: CDF of *U* (Gamma Distribution)

Fig. 3 shows the graphical illustration of the CDF of our model, where we have represented the analytical results in this case. The corresponding noise power at D in the simulation is given by  $^{11}$   $\sigma^2 = N0 + 10\log(BW) + NF (dBm)^2$ .

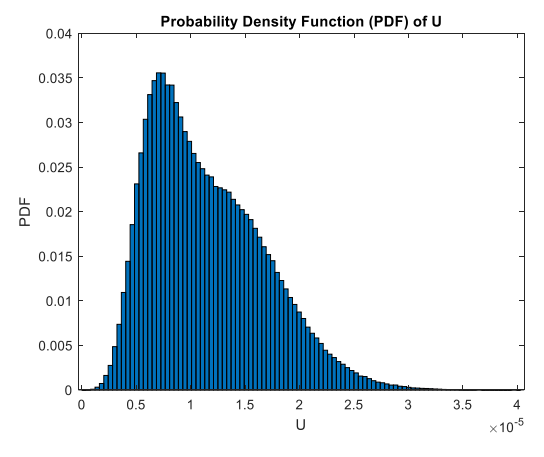


Figure 4: Illustration of the PDF of U for Gamma Distribution

In Fig.4, we discuss the PDF of U for our model for Gamma distribution. Here, the analytical results are plotted as well. These analytical results will be helpful for system designers and network engineers.

## 5. CONCLUSION

In this paper, we have presented a CF-MMIMO model assisted by an IRS panel containing a specific number of PREs serving multiple users, where we evaluated the performance of the network. IRS has been used to facilitate the transmission of signals in this system model. The analysis of different characteristics of our model have been represented and discussed through numerical results. We used different parameters to model and analyze the CDF and PDF for a multi-user scenario with the incorporation of an IRS panel between the source and destination. The OP was also obtained for our model. CF system has a vital role to play in the next generation of wireless communication. Our proposed CF system can be analyzed and modified to create a more extensive structure by increasing the number of IRS panels and the performance for such system can be evaluated. This analysis will help system engineers to design CF systems and evaluate the performances.

### REFERENCES

- J. Zhang, S. Chen, Y. Lin, J. Zheng, B. Ai, and L. Hanzo, "Cell-free massive MIMO: A new next-generation paradigm," IEEE Access, vol. 7, pp. 99 878–99 888 (2019).
- S. Gong, X. Lu, D. T. Hoang, D. Niyato, L. Shu, D. I. Kim, and Y. C. Liang, "Towards smart wireless communications via intelligent reflecting surfaces: A contemporary survey," IEEE Commun. Surveys Tutorials, pp. 1–1 (2020).
- D. Ma, M. Ding, and M. Hassan, "Enhancing cellular communications for UAVs via intelligent reflective surface," in 2020 IEEE Wirel. Commun. and Networking Conf. (WCNC), pp. 1–6 (2020).
- <sup>[4]</sup> Y. Cai, Z. Wei, S. Hu, D. W. K. Ng, and J. Yuan, "Resource allocation for power-efficient IRS-assisted UAV communications," in 2020 IEEE Int. Conf. on Commun. Workshops (ICC Workshops),pp. 1–7 (2020).
- [5] M. Di Renzo, A. Zappone, M. Debbah, M.-S. Alouini, C. Yuen, J. de Rosny, and S. Tretyakov, "Smart radio environments empowered by reconfigurable intelligent surfaces: How it works, state of research, and the road ahead," IEEE J. Sel. Areas Commun., vol. 38, no. 11, pp.2450–2525 (Nov. 2020).
- <sup>[6]</sup> Van Chien, A. K. Papazafeiropoulos, L. T. Tu, R. Chopra, S. Chatzinotas, and B. Ottersten, "Outage Probability Analysis of IRS-Assisted Systems Under Spatially Correlated Channels," IEEE Wireless Communications Letters, (Feb. 2021).
- Y. Jia, C. Ye, and Y. Cui, "Analysis and optimization of an intelligent reflecting surface-assisted system with interference," IEEE Trans. Wireless Commun., vol. 19, no. 12, pp. 8068–8082 (Dec. 2020).
- E. Bjornson, O. Ozdogan, and E. G. Larsson, "Intelligent reflecting surface versus decode-and-forward: How large surfaces are needed to beat relaying," IEEE Wireless Commun. Lett., vol. 9, no. 2, pp. 244–248 (Feb. 2020).
- D. L. Galappaththige, D. Kudathanthirige, and G. A. A. Baduge, "Performance analysis of distributed intelligent reflective surfaces for wireless communications," Available: http://arxiv.org/abs/2010.12543 (Oct. 2020).
- [10] Van Chien, A. K. Papazafeiropoulos, L. T. Tu, R. Chopra, S. Chatzino-tas, and B. Ottersten, "Outage Probability Analysis of IRS-Assisted Systems Under Spatially Correlated Channels," *IEEE Wireless Communications Letters* 10, no. 8, 1815-1819 (2021).
- Do, Tri Nhu, et al. "Multi-RIS-aided wireless systems: Statistical characterization and performance analysis." IEEE Transactions on Communications 69.12, 8641-8658 (2021).
- [12] P. Z. Peebles, Probability, Random Variables and Random Signal Principles, 4th ed. New York, NY, USA: McGraw-Hill Science (2000).
- [13] P. S. Bithas, V. Nikolaidis, A. G. Kanatas, and G. K. Karagiannidis, "UAV-to-ground communications: Channel modeling and UAV selection," IEEE Trans. Commun., vol. 68, no. 8, pp. 5135–5144 (Aug. 2020).
- D. B. da Costa, H. Ding, and J. Ge, "Interference-limited relaying trans-missions in dual-pop cooperative networks over Nakagami-mfading," IEEE Commun. Lett., vol. 15, no. 5, pp. 503–505 (May 2011).
- [15] E. W. Stacy, "A generalization of the gamma distribution," The Annals of Mathematical Statistics, vol. 33, no. 3, pp.1187–1192 (Sep. 1962).